H2A.Bbd: a quickly evolving hypervariable mammalian histone that destabilizes nucleosomes in an acetylation-independent way

José María Eirín-López,*,†,1 Toyotaka Ishibashi,*,1 and Juan Ausió*,2

*Department of Biochemistry and Microbiology, University of Victoria, Petch Building, Victoria, British Columbia, Canada; and †Departamento de Biología Celular y Molecular, Universidade da Coruña, Campus de A Zapateira, Galicia, Spain

ABSTRACT Molecular evolutionary analyses revealed that histone H2A.Bbd is a highly variable quickly evolving mammalian replacement histone variant, in striking contrast to all other histones. At the nucleotide level, this variability appears to be the result of a larger amount of nonsynonymous variation, which affects to a lesser extent, the structural domain of the protein comprising the histone fold. The resulting amino acid sequence diversity can be predicted to affect the internucleosomal and intranucleosomal histone interactions. Our phylogenetic analysis has allowed us to identify several of the residues involved. The biophysical characterization of nucleosomes reconstituted with recombinant mouse H2A.Bbd and their comparison to similar data obtained with human H2A.Bbd clearly support this notion. Despite the high interspecific amino acid sequence variability, all of the H2A.Bbd variants exert similar structural effects at the nucleosome level, which result in an unfolded highly unstable nucleoprotein complex. Such structure resembles that previously described for the highly dynamically acetylated nucleosomes associated with transcriptionally active regions of the genome. Nevertheless, the structure of nucleosome core particles reconstituted from H2A.Bbd is not affected by the presence of a hyperacetylated histone complement. This suggests that replacement by H2A.Bbd provides an alternative mechanism to unfold chromatin structure, possibly in euchromatic regions, in a way that is not dependent on acetylation.—Eirín-López, J. M., Ishibashi, T., and Ausió, J. H2A.Bbd: a quickly evolving hypervariable mammalian histone that destabilizes nucleosomes in an acetylation-independent way. *FASEB J.* 22, 316–326 (2008)

Key Words: chromatin · evolution · sedimentation velocity

IN EUKARYOTES, DNA IS FOUND ASSOCIATED with histones forming a nucleoprotein complex, which is known as chromatin. Chromatin allows for the high extent of compaction of the genomic DNA within the limited space available in the nucleus, and it also provides the support on which most of the DNA metabolic functions (*i.e.,* replication, transcription, and repair) take place (1). Core histones (H2A, H2B, H3,

and H4) provide the protein core about which the DNA is superhelically folded to produce nucleosome core particles (NCPs) that are linked together in the chromatin fiber by short stretches of linker DNA. Linker histones (members of the histone H1 family) bind to these regions, producing an additional folding of the fiber. From the functional point of view, both DNA and histones can be post-translationally modified. DNA is often methylated (2), and histones can undergo an extensive number of post-translational modifications (PTMs) (*e.g.,* acetylation, methylation, phosphorylation, ADP-ribosylation, and ubiquitination) (3, 4) providing chromatin with its epigenetic component (5–7). Because of this tight structural and functional coupling between DNA and histones, it is not surprising that there has been an intimate coevolution of these two chromatin components to the point that it is possible to predict from the sequence of the former the position of the nucleosomes (8). This would also explain why histones are among the most evolutionarily conserved proteins.

In addition to the structural variation imparted by PTMs, histones also consist of replacement variants that provide chromatin with specialized functions and replace canonical histones at different stages of the cell cycle. The primary structure of histone variants can significantly depart from that of the main canonical counterparts, and it is responsible for their dedicated functions. The H1 and H2A histone families contain the largest number of variants (9).

Two highly specialized histone H2A vertebrate variants have been recently described: macro-H2A and H2A.Bbd (10–12). The former is presumably enriched in the female heterochromatic inactivated X-chromosome. In contrast, H2A.Bbd is markedly deficient from the inactive X-chromosome. H2A.Bbd was first identified by *in silico* analysis, and on micrococcal nuclease digestion of chromatin, it was shown to coelute with

---

sucrose gradient-fractionated nucleosomes. Immuno-fluorescence detection revealed an overlapping nuclear distribution of this histone with acetylated H4, suggesting its association with transcriptionally active euchromatic regions of the genome. Indeed, it was later shown that this histone alters the nucleosome conformation and is less tightly bound than the canonical counterpart (13). The nucleosome adopts a more relaxed conformation, which has been attributed to the H2A.Bbd-containing octamers associating with a shorter DNA span of 118 to 130 bp in the nucleosome (14, 15). Fluorescence recovery after photobleaching (FRAP) experiments showed that H2A.Bbd-GFP exchanges from chromatin much more readily compared to the canonical H2A-GFP version (13). This observation was later confirmed using the histone chaperone nucleosome assembly protein I (NAP-I) (16). All this was taken as an indication for a role of this variant in the destabilization of the nucleosome, which is in good agreement with the notion of its involvement in transcription. Domain-swapping experiments indicated that such destabilization involves the whole histone fold domain of this variant (14, 15). The molecular evolutionary analysis presented in this article provides support for this notion and reveals some of the amino acid sequence features that are critical for maintaining the unusually unfolded and unstable nature of the H2A.Bbd-containing nucleosomes. Our data bestow further insight into the rapid evolution of H2A.Bbd (17) and suggest that the main selective constraint in the process is that of maintaining the unfolded conformation of the NCP. Furthermore, such an "open" nucleosome structure is not affected by the acetylation of the rest of the nucleosomal histone complement.

MATERIALS AND METHODS

Sequence alignment

A total of 127 histone H2A sequences belonging to different eukaryotes have been used in our analyses (see Supplemental Table 1), including 2 outgroup sequences from diplomonads. Sequences were retrieved from the GenBank database and subsequently corrected for possible errors in nomenclature. Annotated H2A.Bbd sequences from human were used as a reference in BLAST searches for similar sequences in the complete genomes of other mammals, resulting in the *in silico* identification of this variant in chimpanzee, rhesus monkey, cow, cat, mouse, and rat. Nucleotide coding sequences were aligned on the basis of their translated amino acid sequences using the BIOEDIT (18) and MEGA version 3.1 (19) programs with the default parameters. A bar chart graphical representation was used in order to detail the frequency of each residue at every position of the alignment, using the LogoBar program (20).

Molecular evolutionary analyses

All molecular evolutionary analyses in the present work were carried out using the program MEGA 3.1 (19). The extent of nucleotide and amino acid variation between sequences was estimated by means of the uncorrected differences (*p*-dis-

tance), as this distance is known to give better results than more complicated methods when the number of sequences is large and the number of positions used is relatively small, because of its smaller variance (21). The numbers of synonymous (p_S) and nonsynonymous (p_N) nucleotide differences per site were computed using the modified Nei-Gojobori method (22), providing in both cases the transition:transversion ratio (R). Distances were estimated using the pairwise-deletion option and standard errors were calculated by the bootstrap method with 1000 replicates. The presence and nature of selection were tested by using the codon-based *Z* test for selection, establishing the alternative hypotheses as H_1: $p_N < p_S$ and the null hypothesis as H_0: $p_N = p_S$ (21). The Z-statistic and the probability that the null hypothesis is rejected were obtained, indicating the significance level as **P ($P<0.001$) and *P ($P<0.05$).

Phylogenetic inference

The neighbor-joining tree-building method (23) was used to reconstruct the phylogenetic trees. To assess that our results are not dependent on this choice, phylogenetic inference analyses were completed by the reconstruction of a maximum-parsimony tree (24) using the close-neighbor-interchange (CNI) search method with search level 1 and with 10 replications for the random addition trees option. We decided to combine the bootstrap (25) and the interior-branch test methods (24, 26) in order to test the reliability of the obtained topologies, producing the bootstrap probability (BP) and the confidence probability (CP) values for each internal branch, assuming BP > 80% and CP ≥ 95% as statistically significant (27).

The analysis of the nucleotide diversity across coding regions was performed using a sliding-window approach, by estimating the total (π) and the synonymous (π_S) nucleotide diversity (average number of nucleotide differences per site between two sequences) with a window length of 5 bp and a step size of 1 bp.

Northern dot blot hybridization

Total RNA was extracted from different mouse tissues using Trizol reagent (Gibco BRL, Burlington, ON, Canada), and the purity and concentration were determined by UV absorbance and agarose gel electrophoresis of denatured samples. Total RNA samples (8 μg for *MmH2A.Bbd, MmH2A, Z*; 4 μg for *MmH4*; or 1.5 μg for 18S ribosomal) were dissolved in 10 mM NaOH, 1 mM EDTA and transferred to Zeta-Probe GT blotting membrane (Bio-Rad, Mississauga, ON, Canada) using a Bio-Dot Microfiltration Apparatus (Bio-Rad) following the manufacturer's directions, then cross-linked to the membrane with UV (120,000 μJ). Polymerase chain reaction (PCR) products run on agarose gels gave single bands of the expected sizes, which were excised, purified using the QIAquick Gel extraction kit (Qiagen, Mississauga, ON, Canada), and sequenced as described above to confirm their identity. The purified PCR products were labeled with the Random Primer DNA Labeling System (Invitrogen, Burlington, ON, Canada) following the Standard Labeling protocol to produce probes. Hybridization of ~10^6 cpm ^{32}P-labeled cDNA probes in PerfectHyb™ Plus buffer (Sigma, Oakville, ON, Canada) were incubated overnight with the blots. Membranes were then washed to high stringency, exposed, and analyzed (28).

Protein expression

The coding region of *MmH2A.Bbd* was cloned into the pET11 expression vector (Novagen, EMD Biosciences, La Jolla, CA,

USA). For protein expression, it was introduced into BL21 (DE3) *Escherichia coli* (Novagen, EMD Biosciences), and the bacteria grown in 2 L LB medium. Cells were grown to an A_{600} of 0.8, and isopropyl β-D-thiogalactoside was added to a final concentration of 1 mM. Cells were harvested after 3 h by centrifugation at 5000 g for 10 min at 4°C. Cell pellets were resuspended in 10 ml ice-cold binding buffer (50 mM Na_2HPO_4, pH 7.8) and sonicated with 20 bursts of 10 s each. Cell lysates were centrifuged at 29,000 g for 30 min. Cell pellets were solubilized in unfolding buffer (8 M urea, 50 mM Na_2HPO_4, pH 7.8) and centrifuged for 1 h at 20,000 g. Soluble fractions were loaded on to Hitrap SP HP column (GE Healthcare Biosciences, Quebec, QC, Canada). After being washed, the fraction was collected with 40 ml of a linear gradient of 0–1 M NaCl in buffer 8 M urea, 50 mM Na_2HPO_4. The eluted MmH2A.Bbd protein was dialyzed against 5 mM 2-mercaptoethanol and used in the subsequent experiments.

Chicken histones

Chicken erythrocyte (nonacetylated, control) histones were prepared as described elsewhere (29). In brief, chicken erythrocyte chromatin (fraction SE) was stripped of linker histones using CM C-25 Sephadex in 0.35 M NaCl, 10 mM Tris-HCl (pH 7.5) buffer (29) and loaded onto a hydroxyapatite column that had been previously equilibrated with 350 mM NaCl, 20 mM Na-phosphate (pH 6.8) buffer. Histone octamers were subsequently eluted in 2.2 M NaCl, 20 mM Na-phosphate (pH 6.8) buffer. Chicken acetylated histones (with an average of 13 acetylated sites per nucleosome) were prepared in a similar fashion but were obtained from MSB chicken erythroleukemic cells (30).

Nucleosome core particle reconstitution

A histone protein titration was carried out using SDS-PAGE to ensure that all histones in the final mixture were present in equimolar amounts. The histone mixture thus obtained was dialyzed overnight against 2.0 M NaCl, 10 mM Tris-HCl (pH 7.5), 10 mM β-mercaptoethanol, and 0.1 mM EDTA at 4°C, and was mixed with 146 bp random sequence chicken DNA in the same buffer at a histone:DNA ratio of 1.13:1.0 (w/w). Nucleosome core particle reconstitution was carried out using salt gradient dialysis (29, 31). The integrity of the core particles was analyzed by 4% native PAGE and sedimentation velocity in the analytical ultracentrifuge (see below).

Analytical ultracentrifugation

Reconstituted MmH2A.Bbd NCPs were dialyzed against buffers of varying ionic strengths and were subjected to analytical ultracentrifuge analysis as described elsewhere (29). Briefly, sedimentation velocity runs were performed in a Beckman XL-I analytical ultracentrifuge (Beckman-Coulter Instruments, Fullerton, CA, USA) in an An-55 Al aluminum rotor using cells with double sector aluminum-filled Epon centerpieces. A value of 0.650 cm^3/g was used for the partial specific volume of NCP (29). Absorbance scans were routinely obtained at 260 nm and the boundaries were analyzed as described elsewhere (32) with the help of UltraScan 8.0 sedimentation data analysis software (Borries Demeler, Missoula, MT, USA).

MgCl$_2$ nucleosome solubility

Reconstituted H2ABbd-containing NCPs were incubated with increasing concentrations of $MgCl_2$ for 50 min at 4°C and centrifuged at 16,000 g at the same temperature. The absorbance of the NCP remaining in solution at each $MgCl_2$ concentration was measured at 260 nm. The data presented here represent the average of three independent determinations.

Polyacrylamide gel electrophoresis (PAGE)

Acetic acid–urea (AU) -PAGE was carried out as described elsewhere (33). SDS-PAGE was performed according to Laemmli (34). Native-(4.5%)-PAGE (acrylamide:bis-acrylamide 29:1, w/w) for nucleosome analysis was carried out in 20 mM sodium acetate, 1 mM EDTA, 20 mM Tris-HCl (pH 7.2), E buffer as described elsewhere (35, 36).

RESULTS

Histone H2A.Bbd is a highly variable histone H2A variant

On quick inspection, histone H2A.Bbd contains several characteristic features that set it apart from canonical H2A. For instance, the presence of a continuous stretch of arginines and the conspicuous absence of lysines in its N-terminal tail, as well as the absence of a C-terminal tail, have already been documented. Differences in the very last segment of the docking domain that is responsible for interactions of H2A with H3 in the NCP and the lack of residues that contribute to the NCP "acidic patch" have also been described. There is only one lysine in human H2A.Bbd compared to 14 in canonical H2A (7, 10, 14).

In the present work, we have analyzed H2A.Bbd histones identified *in silico* from genome databases (except for human H2A.Bbd, which is currently annotated), resulting in the identification of this variant in chimpanzee, rhesus monkey, cow, cat, mouse, and rat. As a reference for this group of mammals, H2A.Bbd sequences were compared with their canonical H2A counterpart in order to investigate in detail the extent of variation between these two H2As.

The logos analysis below the sequence alignments shown in **Fig. 1** underscores the high extent of variability between H2A and H2A.Bbd. However, despite this variability in the H2A.Bbd amino acid sequence, there are highly conserved residues (the same for all H2ABbd sequences) at 15 different amino acid positions (indicated by a black star below the corresponding alignment positions in Fig. 1). At these 15 positions, a given amino acid from H2A has been replaced by a different conserved one in all H2A.Bbd variants, suggesting that this event is likely driven by some kind of selective constraint.

Although some positions are conserved between H2A and H2A.Bbd, especially in the α-helix 2 of the histone fold (37), there is an extensive degree of divergence. A closer examination of the changes exhibited by H2A.Bbd when compared to H2A revealed that 14 of the 23 (60.87%) substitutions involving a basic amino acid in H2A are replaced by a nonbasic residue in H2A.Bbd (solid arrowheads above the alignment in Fig. 1), while 6
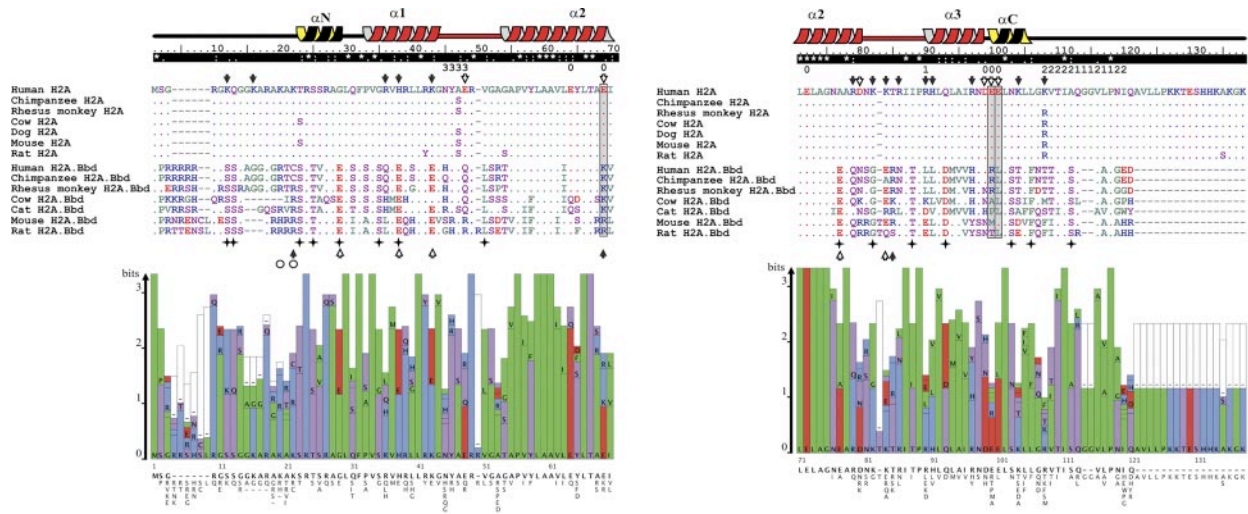
Figure 1. Amino acid alignment of the canonical H2A and the H2A.Bbd proteins. The secondary structure for the H2ABbd variant is represented above the alignment. White asterisks, colons, and dots above the alignment indicate positions where residues are totally conserved, highly conserved, or poorly conserved, respectively. Gaps and matching residues are indicated by dashes and dots, respectively, in the alignment. The residues of H2A that are part of the nucleosome acidic patch are shaded in the alignment; black stars denote positions with fixed changes in H2A.Bbd. Solid and open arrowheads above the alignment indicate positions where basic and acidic residues in H2A are replaced by any other type of residue in H2A.Bbd, respectively and excluding gap positions. Numbers 0, 1, 2, and 3 above the alignment indicate those residues involved in internucleosomal contacts, H2A/H3, H2A/H4, and H2A/H2A interactions, respectively. Solid and open arrowheads below the alignment indicate positions where basic and acidic residues in H2A.Bbd, respectively, are replacing any other type of residue in H2A and excluding gap positions. Open circles below the alignment indicate changes from lysines in H2A to arginines in H2A.Bbd. The bar plot represents the amino acid variability at each position of the alignment, with the size of the bars proportional to the frequency for a given amino acid. The overall height of the bars is proportional to the conservation of the site. Colors have been assigned to the amino acids according to their physical and chemical structural characteristics (red, acidic; blue, basic; nonpolar hydrophobic, green; polar hydrophylic, purple).

of the 8 (75.0%) substitutions involving acidic residues in H2A are replaced by a nonacidic residue in H2A.Bbd (open arrowheads above the alignment in Fig. 1). When doing a similar comparison in reverse, 3 of the 5 (60.0%) substitutions involving a change in any residue (except basic ones) in H2A are replaced by a basic residue in H2ABbd (solid arrowheads below the alignment in Fig. 1), while 5 of 5 (100%) substitutions involving a change in any residue (except acidic ones) in H2A are replaced by acidic residues in H2A.Bbd (open arrowheads below the alignment in Fig. 1). Thus, there appears to be a certain bias toward the loss of basic residues in H2A.Bbd compared with H2A (with the exception of the arginine tracts in the N-terminal region, which most likely correspond to sequence insertions and deletions). Interestingly, whenever basic residues are maintained in H2A and H2A.Bbd, the latter exhibits a preference for arginine over lysine. Equally noticeable is the loss of the acidic residues of H2A (E69, E100, and E101, which contribute to the nucleosome acidic patch; ref. 38) and which are replaced by basic and nonpolar residues in H2A.Bbd. These residues play an important role in the internucleosomal interactions within the chromatin fiber (see below).

Alterations in the amino acid sequence also affect sites that are involved in intranucleosomal histone-histone interactions (39). These amino acid positions have been indicated in Fig. 1, with numbers 1, 2, and 3 corresponding to alterations affecting H2A/H3, H2A/H4, and H2A/H2A interactions, respectively. Four of the 6 positions

involved in H2A/H3 interactions are disturbed in H2A.Bbd, as well as 5 of 7 involved in H2A/H4, and 3 of 4 involved in H2A/H2A interactions.

In an attempt to gain further insight into the evolutionary processes underlying the H2A.Bbd variability, we analyzed the total and synonymous nucleotide variation across the H2ABbd molecule (in comparison with H2A) within mammals (**Fig. 2**). While the total nucleotide variation shown by H2ABbd is higher than the variation observed for H2A (Fig. 2A), the silent variation is similar in both histones (Fig. 2B). This suggests that the higher variation observed for H2A.Bbd is the result of a higher occurrence of nonsynonymous changes, which appear to affect the region comprising the histone fold to a lesser extent than the rest of the protein, in agreement with the results shown in Fig. 1. This is most likely because of structural constraints required for the histone fold interactions involved in the formation of the H2A.Bbd-H2B dimer, regardless of the variation in the sites affecting other histone-histone interactions that are critical for the intra- and internucleosomal stability and folding described above.

Despite all the information provided in this section, the evolutionary constraints operating on H2A.Bbd sequence intravariability and intervariability in relation to other H2A histones (especially at the protein level) still remains an open issue. Nevertheless, whatever the mechanism is, our results conclusively show that this must be quite different from the archetypical negative
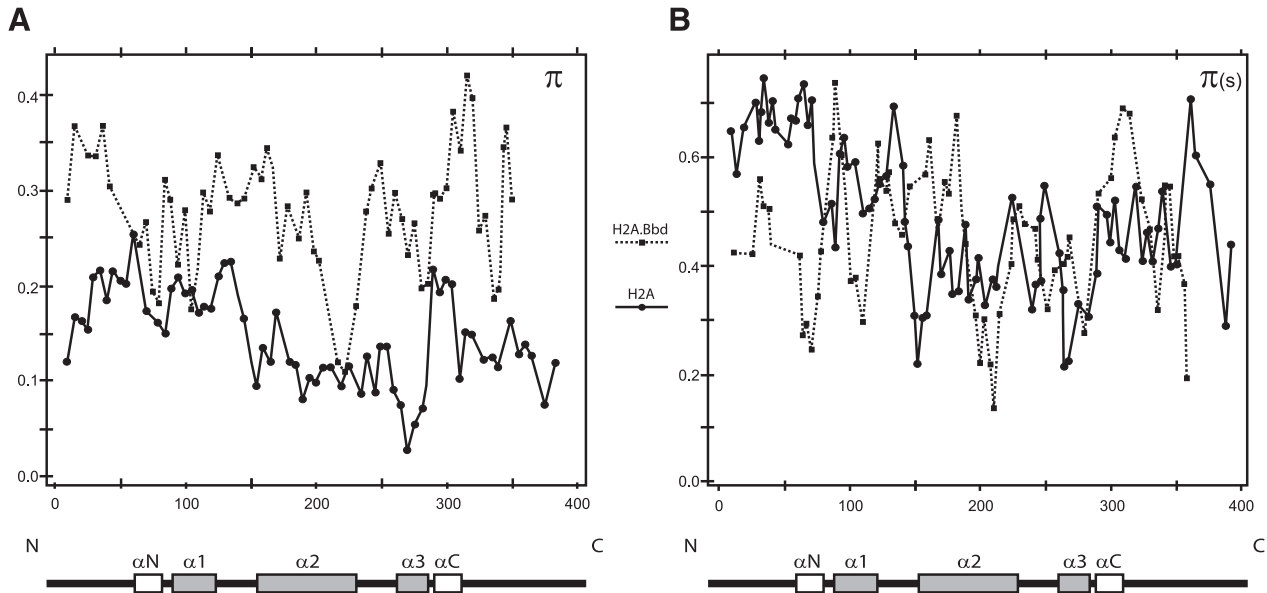
Figure 2. Total (π) (*A*) and synonymous (πs) (*B*) nucleotide diversity (expressed as the average number of nucleotide differences per site) across the coding regions of H2A and H2A.Bbd genes. The diversity values were calculated using a sliding-window approach with a window length of 5 bp and a step size of 1 bp. The corresponding secondary structure (for H2A.Bbd) is represented below the plots, scaled to the size of the graphs.

selection process, which is responsible for maintaining the protein structure of all of the other core histones.

Histone H2A.Bbd: a primitive histone H2A variant of monophyletic origin in mammals

To set the analysis of the histone H2A.Bbd within a broader evolutionary context, a phylogenetic tree, including all other H2A variants was reconstructed (**Fig. 3**). Consistent with previous phylogenetic analyses (17, 40) the topology thus obtained indicates a monophyletic origin for all H2A variants, with the exception of H2A.X, whose recurrent evolutionary origin across eukaryotic evolution has been previously described (17). In addition, two main conclusions can be drawn from the tree shown in Fig. 3. First, the H2A.Bbd lineage is the variant with the highest levels of divergence with respect the other H2A lineages, as evidenced by the larger tree branches for each of the H2ABbd sequences analyzed (corresponding to higher levels of residue changes per residue position). Second, the tree topology indicates that the differentiation of the H2A.Bbd lineage appears to have occurred very early in H2A evolution. The apparent discrepancy between this observation and the inability of the *in silico* analysis to identify the presence of this variant in invertebrate and vertebrate organisms other than mammals will be discussed later.

Sequence variability between and within H2A and H2A.Bbd variants

To better ascertain the origin of the H2A.Bbd variation observed in the phylogenetic tree (Fig. 3), we analyzed the evolutionary distances both at the amino acid and

the nucleotide level within each of the H2A variants. As can be seen in **Table 1**, in terms of amino acid replacements, histone H2A.Bbd is again the protein with the highest level of variation among all H2A histones. Such amino acid variation is in contrast with the protein conservation that characterizes histones. Furthermore, at the nucleotide level, H2A.Bbd displays the lowest levels of both total nucleotide variation and synonymous nucleotide variation (*Z* test 5.230) among H2A histones (*Z* test ~20,000) (Table 1), which is opposite to the common trend in histones, which are characterized by their high levels of nucleotide synonymous variation. Despite the departure from the conservation of the protein sequence, the results for the *Z* test of selection on H2A.Bbd reveal that the overall synonymous variation is still significantly higher than the nonsynonymous variation. This suggests the presence of purifying selection acting on this variant as is also the case for the remainder of the H2A variants and disregards any possibility of an hypothetical switch of the H2A.Bbd lineage toward some kind of adaptive process.

The characterization of the extent of variation within members of the histone H2A.Bbd variant family itself was carried out by pair-wise comparison of all the sequences available (Fig. 1 and **Table 2**). Such analysis revealed closer relationships in closely phylogenetically related organisms (*i.e.*, human and chimpanzee, or mouse and rat), as is to be expected. However, and quite unexpectedly, an extreme divergence of murine (mouse and rat) H2A.Bbd was observed with respect to any of the other mammalian H2A.Bbd sequences from different taxonomic groups.

Analysis of the sequence variation between H2A variants (**Table 3**) was also an indicator that H2A.Bbd is
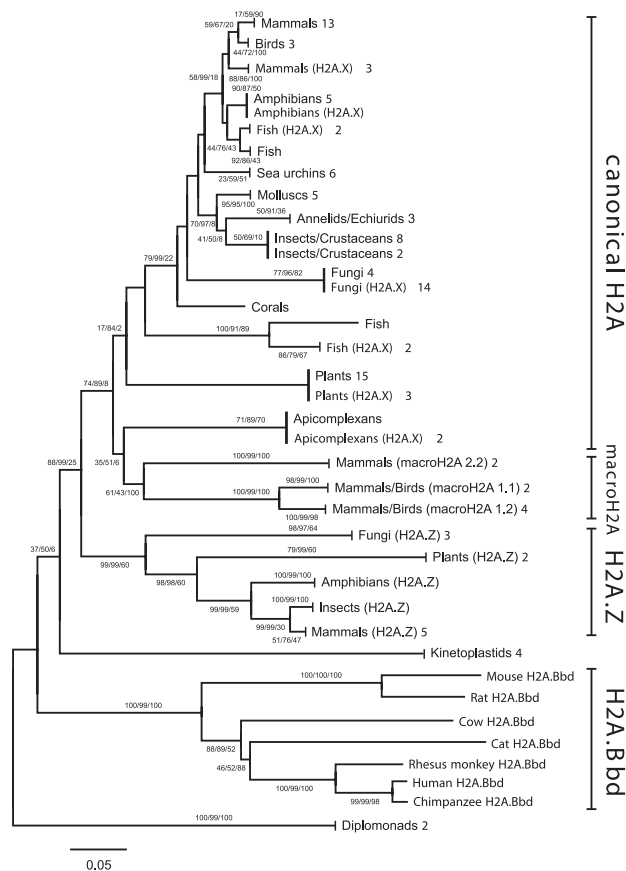
Figure 3. Phylogenetic tree reconstructed from amino acid H2A. Sequences representing canonical and variant types are indicated in the right hand side of the topology (except for H2A.X variants, which are indicated in italics). A total of 127 amino acid sequences were used in the reconstruction of the phylogeny (70 from canonical H2A, 8 from macro H2A, 30 from H2A.X, 12 from H2A.Z, and 7 sequences corresponding to H2A.Bbd), and the tree was rooted with H2A sequences corresponding to two different *Giardia* species. The tree was built using the neighbor-joining method, and the confidence levels for the groups defined in the topology were assessed by bootstrap and interior branch tests (1000 replicates). The tree was also reconstructed using maximum parsimony, resulting in a similar topology to that obtained with the neighbor-joining method (suggesting that the topology obtained is not dependent on the tree-building method used). Numbers in interior branches indicate the confidence values obtained for bootstrap, interior branch test, and the bootstrap value for the maximum parsimony reconstruction for a given node, respectively. These values are shown only when either the bootstrap or the interior branch test result is higher than 50%.

the type showing the highest levels of divergence (p-distance values) with respect to other H2A histones, both at the nucleotide and amino acid level. These values are in all instances higher than those observed between H2A.X and any other H2A histone. This is important considering that H2A.X shows the highest levels of nucleotide nonsynonymous variation, probably due to its recurrent coevolution with canonical H2A histones, which results in a phylogenetic interspersed pattern (Fig. 3) (40). In addition, H2A.Bbd does not show any preferential similarity for any other H2A variant. In other words, H2A.Bbd is equally unrelated to any other H2A type to almost exactly the same extent.

H2A.Bbd expression in mouse tissues

As can be seen in Fig. 1 and Table 2, the human and mouse H2A.Bbd represent the two most different forms of this histone variant. Among other important differences (see above), mouse H2A.Bbd lacks the N-terminal arginine cluster, which is characteristic of the mammalian H2A.Bbd histone. To date, expression of H2A.Bbd has been demonstrated only in humans (10). Given the extensive departure of the mouse H2A.Bbd amino acid sequence identified by *in silico* analysis (Fig. 1) we decided to check whether the identified sequence indeed corresponded to an expressed histone H2A variant to eliminate the possibility of a pseudogene origin. To this end, we purified mRNA from different mouse tissues and performed Northern dot blot analysis (**Fig. 4**). The results show that an mRNA corresponding to the sequence identified *in silico* is transcribed. Furthermore, as with mouse core histones (histone H4) and other mouse histone H2A variants (H2A.Z), the highest mRNA levels were detected in testes. The presence of high levels of core histones in unfractionated testes can be attributed to the large number of cells at different stages of mitosis and meiosis in this tissue. The high presence of a replacement histone variant such as H2A.Z may be the result of the important involvement of this variant in sex chromosome inactivation during spermatogenesis (41). Like histone H2A.Z, H2A.Bbd was isolated from a poly(A)+ mRNA fraction as occurs with most replacement histone variants (17); nevertheless, the reason for

TABLE 1. *Average amino acid and nucleotide differences per site in H2A genes and standard errors calculated using the bootstrap method (1000 replicates)*

	pAA[a]	pNT[b]	pS[c]	pN[d]	R[e]	Z test	P value
H2A	0.251 ± 0.019	0.342 ± 0.014	0.669 ± 0.009	0.207 ± 0.015	0.7	24.372	0.000
H2A.Z	0.236 ± 0.023	0.338 ± 0.015	0.699 ± 0.013	0.222 ± 0.019	0.8	19.282	0.000
H2A.X	0.310 ± 0.021	0.379 ± 0.014	0.689 ± 0.010	0.254 ± 0.017	0.8	23.083	0.000
MacroH2A	0.268 ± 0.014	0.283 ± 0.010	0.518 ± 0.015	0.113 ± 0.008	0.9	24.200	0.000
H2A.Bbd	**0.358 ± 0.029**	**0.277 ± 0.015**	**0.414 ± 0.027**	**0.227 ± 0.021**	**0.8**	**5.230**	**0.000**
Overall average	0.338 ± 0.020	0.399 ± 0.013	0.695 ± 0.009	0.269 ± 0.015	0.7	22.291	0.000

[a]Amino acid differences per site (p-distance). [b]Nucleotide differences per site (p-distance). [c]Synonymous differences per site. [d]Nonsynonymous differences per site. [e]Transition:transversion ratio

TABLE 2. *Average amino acid (lower diagonal) and nucleotide (upper diagonal) differences per site (p-distance) between species in the case of histone H2ABbd*

	Human	Chimpanzee	Rhesus monkey	Cow	Cat	Mouse	Rat
Human	—	0.011	0.078	0.279	0.260	**0.357**	**0.360**
Chimpanzee	0.026	—	0.078	0.282	0.266	**0.360**	**0.363**
Rhesus monkey	0.122	0.130	—	0.267	0.257	**0.381**	**0.355**
Cow	0.358	0.367	0.330	—	0.264	**0.355**	**0.352**
Cat	0.336	0.345	0.372	0.413	—	**0.366**	**0.363**
Mouse	**0.420**	**0.429**	**0.429**	**0.477**	**0.509**	—	**0.141**
Rat	**0.429**	**0.429**	**0.438**	**0.477**	**0.509**	**0.165**	—

the enhanced occurrence of H2A.Bbd in testes remains to be determined.

Effects of histone H2A.Bbd hypervariabilty on NCP conformation and stability: role of histone acetylation

Using as background the information provided in the previous sections, we next wanted to address the following questions: *1)* Does the high interspecies H2A.Bbd variability affect the conformation of the NCP in different ways? *2)* What are the structural implications of this variability for NCP stability? *3)* Is the conformational effect of H2A.Bbd at the NCP level affected by histone acetylation? To experimentally address these questions, we reconstituted nucleosomes with mouse H2A.Bbd (**Fig. 5**) and compared their conformation and stability to those consisting of human H2A.Bbd.

Figure 6 shows that despite the extensive amino acid sequence variability between mouse and human H2A.Bbd, NCPs reconstituted with either one of them exhibit a very similar salt-dependent hydrodynamic behavior, which is consistent with an extended conformation (13). Furthermore, these particles are very labile (**Fig. 7**). At ~600 mM NaCl (Fig. 7), ~80% of the NCPs exist as a mixture of subnucleosomal particles deficient in 1 or 2 histone H2A.Bbd dimers. This is the result of a reduced internucleosomal histone-histone interaction that affects the H2A.Bbd-H2B and H3-H4 interfaces within the histone core (14). These results are in excellent agreement with the predictions of our molecular evolutionary analyses described above.

Interestingly, the ionic-strength-dependent conformational changes of the H2A.Bbd NCPs are highly reminiscent of those of native NCPs consisting of hyperacetylated histones (42) (**Fig. 8***A*) and like acetylated nucleosomes exhibit a slightly higher MgCl$_2$ solubility (43) (Fig. 8*B*). Moreover, the conformation of the NCPs reconstituted from H2A.Bbd is not affected by the presence of a hyperacetylated histone complement (Fig. 8*A*).

DISCUSSION

The phylogenetic analysis of histone H2A variants using the mammalian sequence information obtained from *in silico* analysis (Figs. 1 and 2) unambiguously identifies histone H2A.Bbd as one of its most divergent members with a primitive origin (Fig. 3). H2A.Bbd branch lengths seem to be only comparable with H2A proteins from kinetoplastids, which is quite unexpected taking into account that H2A.Bbd can only be identified in mammals. The high extent of divergence of histone H2A .Bbd is most likely hindering its identification in the phylogeny, giving it the appearance of a variant with a primitive evolutionary origin when indeed it is only found in mammals. Nevertheless, the rapidly evolving nature of this histone variant is striking considering that histones are among the most highly evolutionarily conserved proteins (44).

Our results indicate that, despite a relative increase in the number of nonsynonymous nucleotide substitutions observed with H2A.Bbd (Table 1), the overall synonymous variation is still significantly higher as revealed by the *Z* test of selection. Interestingly the magnitude of the nonsynonymous variability appears to be lower in the protein region comprising the histone fold, which contains highly conserved amino acid positions (including the characteristic glutamic acids) (see stars and lower arrowheads in Fig. 1) that provide the structural signature to the H2A.Bbd protein members and are responsible for the destabilization of the internucleosomal interactions and the unfolded conformation (Figs. 6 and 7).

TABLE 3. *Average amino acid (lower diagonal) and nucleotide (upper diagonal) differences per site (p-distance) between H2A variants*

|	H2A	H2A.Z	H2A.X	MacroH2A	H2ABbd
H2A	—	0.463	0.377	0.413	**0.512**
H2A.Z	0.432	—	0.468	0.482	**0.558**
H2A.X	0.278	0.438	—	0.444	**0.536**
MacroH2A	0.357	0.489	0.379	—	**0.540**
H2A.Bbd	**0.619**	**0.663**	**0.624**	**0.659**	—

The FASEB Journal
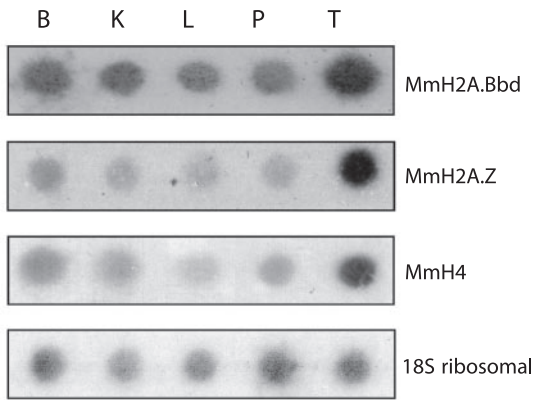
Figure 4. Transcription of mouse (*Mus musculus*) H2A.Bbd in different tissues. Analysis of the occurrence of H2A.Bbd mRNA in comparison to other mice histone mRNAs in different tissue samples using Northern blot analysis. N, sample containing no RNA; B, brain; K, kidney; L, liver; P, prostate; T, testis.

The only other known major chromosomal proteins with a fast evolution rate are protamines (45–48). Protamines are a group of relatively small arginine-rich proteins that replace histones during spermiogenesis in different groups of invertebrate and vertebrate organisms (45). It has been shown that, in mammals, positive Darwinian selection is the main driving force behind this rapid evolution, likely as a result of sexual selection (45). In this instance, it was found that the rate of nonsynonymous nucleotide substitution is significantly higher than
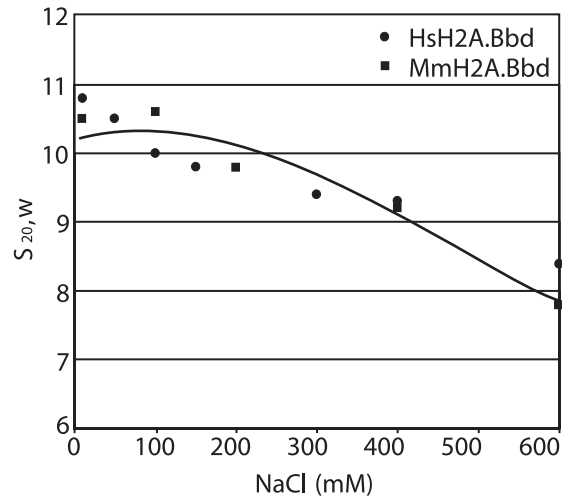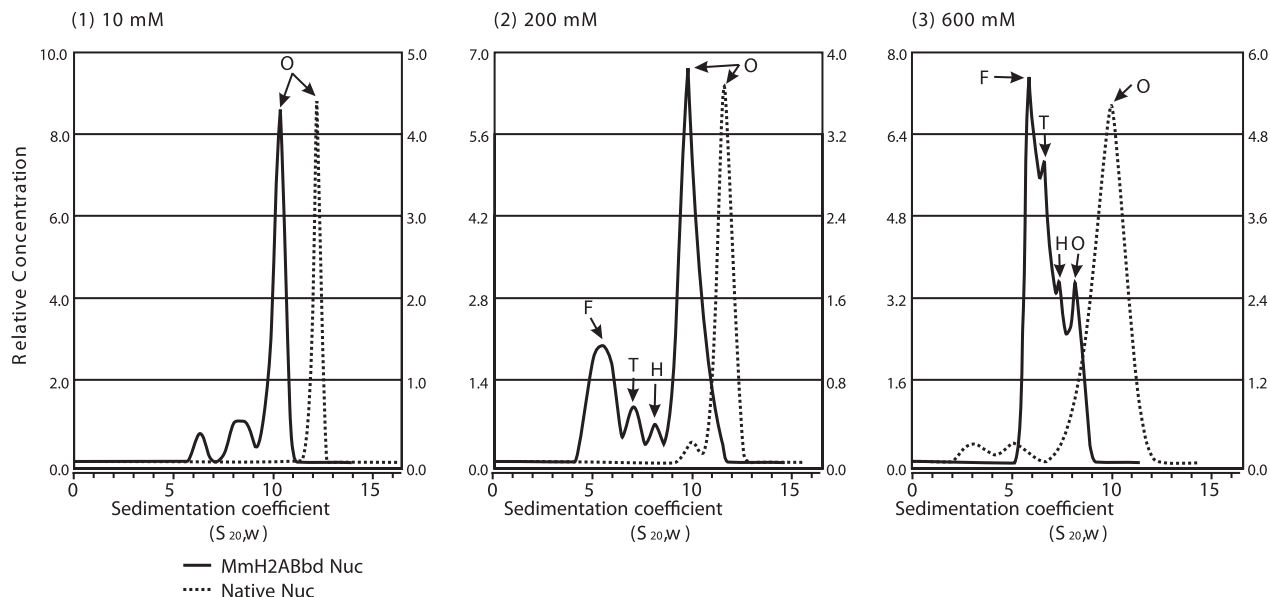

Figure 6. Ionic strength-dependence of the sedimentation coefficient ($s_{20,w}$) of nucleosome core particles reconstituted with H2A.Bbd. Nucleosome core particles reconstituted with mouse H2A.Bbd (MmH2A.Bbd) were dialyzed against 20 mM Tris-HCl, 0.1 mM EDTA (pH 7.5) buffer consisting of different NaCl concentrations and analyzed by analytical ultracentrifuge at 44,000 rpm and 20°C. The data for human H2A.Bbd reconstituted nucleosome core particles were taken from ref. 13.

the rate of synonymous nucleotide substitution (48). As pointed out by these authors, the forces of negative and positive selection operate simultaneously in rapidly evolving genes. The molecular evolutionary data described
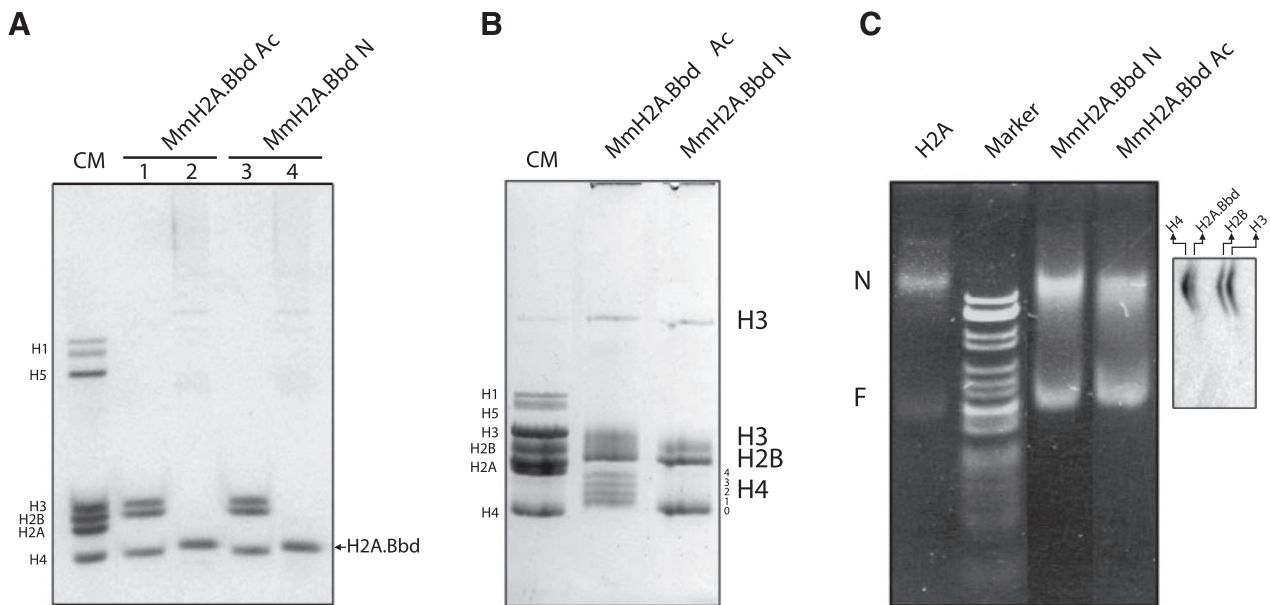
Figure 5. Electrophoretic analyses of different stages of the H2A.Bbd-NCP reconstitution. *A)* SDS-PAGE of H2A.Bbd (lanes 2, 4) and the complement (H2B/H3/H4) of native nonacetylated (lane 1) and acetylated (lane 3) octameric core histones used in the reconstitution. *B)* AUT-PAGE of the histones from H2A.Bbd-reconstituted octamers consisting of an acetylated (MmH2A.Bbd Ac) or native nonacetylated (MmH2A.Bbd N) histone core complement. Histone H2A.Bbd runs close to histone H2B but does not stain well in this type of gel. CM; chicken erythrocyte histones used as a marker. *C)* Native-PAGE of nucleosome core particles reconstituted from 146 bp random sequence chicken DNA and histone octamers consisting of canonical H2A (H2A); H2A.Bbd and a nonacetylated histone complement (MmH2A.Bbd N); H2A.Bbd and acetylated histone complement (MmH2A.Bbd Ac). The marker is a *Cfo*I-digested pBR322 plasmid DNA. The right-hand side shows a two-dimensional electrophoretic analysis of the sample shown in lane MmH2A.Bbd N. A strip of the gel in *C* corresponding to this lane was overlaid and electrophoretically run in the second dimension using SDS-PAGE.

Figure 7. Ionic strength-destabilized organization of nucleosome core particles reconstituted with H2A.Bbd. The graphs show plots of the relative sample concentration *vs.* the sedimentation coefficient at three different NaCl concentrations (10, 200, and 600 mM). Data were obtained using the histogram envelope analysis from the UltraScan software described in Materials and Methods. The right- and left-hand units in each plot correspond to the relative concentrations of H2A.Bbd-reconstituted and native NCPs, respectively. O, NCP consisting of a full histone octamer; H, NCP consisting of a histone hexamer (deficient in one H2A-H2B dimer); T, NCP consisting of a histome tetramer (lacking two H2A-H2B dimers); and F, free (fully dissociated) 146 bp DNA.

here indicate that, in contrast to protamines, histone H2A.Bbd members are subject to the purifying selection process, which is characteristic of histones (49).

The comparison of the biophysical characteristics of NCPs reconstituted with two of the most divergent H2A.Bbd histone members (human and mouse) (Fig. 8) can provide some insight into the selective forces driving the evolution of this H2A variant. Its poly(A)+ nature (Fig. 4) suggests that indeed this is a replacement variant that is incorporated into chromatin outside of the S-phase of the cell cycle in order to "replace" another histone H2A within preassembled NCPs. The conformational results (Fig. 8) indicate that such replacement imparts to the NCP an unfolded highly unstable conformation that is independent of the hypervariable interspecies sequence variability. Therefore, the maintenance of such unusual NCP conformation appears to be the main structural and functional constraint behind the selection process.

The "open" dynamic conformational transition resulting from H2A.Bbd incorporation to the NCP supports the notion that this variant may be involved in transcription, and it is probably present in the euchromatin regions of the genome (10). Interestingly, it has been shown that NAP-I can mediate an efficient exchange of H2A.Bbd-H2B dimers from NCPs *in vitro* (16). NAP-I has been shown to play an important role in the chromatin remodeling involved in transcriptional activation (50).

Furthermore, it has been shown that the chromatin occurrence of H2A.Bbd overlaps with regions containing acetylated H4 (10). Global acetylation of core histones also plays a very important role in the modulation of gene expression (51) and has been shown to

change the NCP conformation (42) partially releasing the flanking DNA regions of the NCP (3, 52, 53). The salt-dependent conformational change similarity between NCPs reconstituted with H2A.Bbd and native acetylated nucleosomes (Fig. 8) is quite interesting. Equally striking is the lack of conformational change by histone acetylation on H2A.Bbd-containing NCPs (Fig. 8). These results suggest that like global histone acetylation, H2A.Bbd may participate in transcription by relaxing the NCP conformation, thus providing an alternative device to unfold chromatin structure. Nevertheless, unlike the highly dynamic (reversible) nature of histone acetylation (54), H2A.Bbd would impart a more permanent NCP altered structure that could only be reverted by a chromatin-remodeling process involving H2A-H2B exchange.

The distinctive amino acid sequence features that allow the clear distinction of H2A.Bbd from other histone H2A variants (Fig. 1) also have implications for the internucleosomal interactions within the chromatin fiber. Histone H2A is the main contributor of acidic amino acids to the "acidic patch" of the nucleosome (38, 55). This acidic patch has been shown to interact with the basic residues of the N-terminal tail of histone H4 in the neighboring nucleosome, an interaction that plays an important role in the higher-order folding of the nucleosome arrays (38, 56) (and chromatin fibers). Therefore, abolishment of these acidic amino acids in H2A.Bbd, as has been described in the previous section, has implications for the folding of nucleosome arrays, presumably resulting in an unfolded state. Such nucleosome fiber unfolding would explain the higher efficiency of p300- and Gal4-VP16-activated transcription on H2A.Bbd nucleosome arrays (57).

A

B
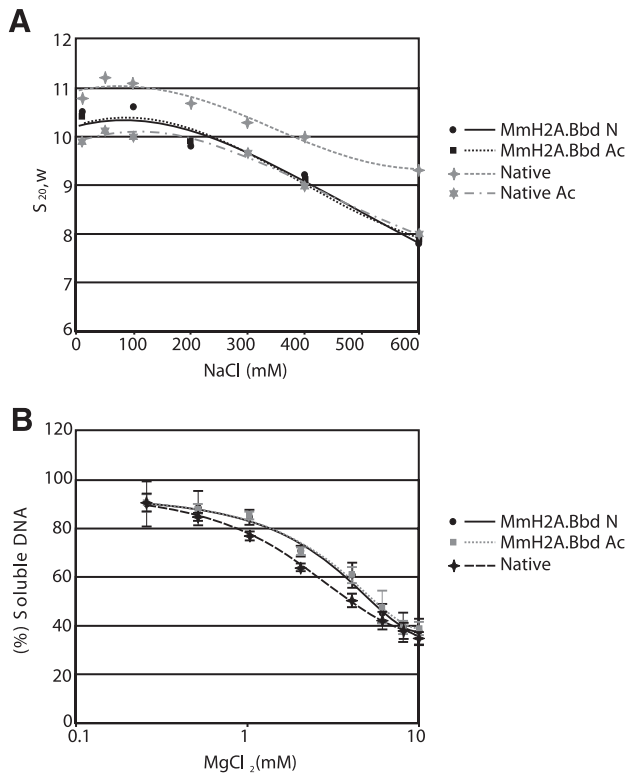
Figure 8. H2A.Bbd unfolds the NCP in a way that resembles the unfolding produced by histone acetylation. *A)* Ionic strength dependence of the sedimentation coefficient ($s_{20,W}$) of NCPs reconstituted with mouse H2A.Bbd using either a nonacetylated (MmH2A.Bbd N) or an acetylated (MmH2A.Bbd Ac) histone complement (see Fig. 5*B*). The data are compared to the results obtained with native NCPs and to native acetylated NCPs (46). *B)* $MgCl_2$ solubility of MmH2A.Bbd N and MmH2A.Bbd Ac reconstituted NCPs in comparison to NCPs reconstituted with a native nonacetylated histone H2A complement.

The very low abundance of H2A.Bbd within the cell makes it difficult to identify the genes or discrete chromatin domains that are preferentially targeted by this variant. Comparative sequence analyses, such as were carried out here, should make it possible to design more specific antibodies to this purpose unless, and the possibility exists, that this variant is promiscuously distributed in transcriptionally active domains as its original ambiguous name "Barr body deficient" seems to indicate. [FJ]

REFERENCES

1. Van Holde, K. E. (1988) *Chromatin.* Springer-Verlag, New York
2. Bernstein, B. E., Meissner, A., and Lander, E. S. (2007) The mammalian epigenome. *Cell* **128,** 669–681
3. Ausió, J., and Abbott, D. W. (2004) The role of histone variability in chromatin stability and folding. In *Chromatin Structure and Dynamics: State-of-the-Art* (Zlatanova, J., and Leuba, S. H., eds) pp. 241–290, Elsevier, New York
4. Peterson, C. L., and Laniel, M. A. (2004) Histones and histone modifications. *Curr. Biol.* **14,** R546–R551
5. Imhof, A. (2006) Epigenetic regulators and histone modification. *Brief. Funct. Genomic. Proteomic.* **5,** 222–227
6. Kouzarides, T. (2007) Chromatin modifications and their function. *Cell* **128,** 693–705
7. Strahl, B., and Allis, C. D. (2000) The language of covalent histone modifications. *Nature* **403,** 41–45
8. Segal, E., Fondufe-Mittendorf, Y., Chen, L., Thastrom, A., Field, Y., Moore, I. K., Wang, J. P., and Widom, J. (2006) A genomic code for nucleosome positioning. *Nature* **442,** 772–778
9. Ausio, J. (2006) Histone variants—the structure behind the function. *Brief. Funct. Genomic. Proteomic.* **5,** 228–243
10. Chadwick, B. P., and Willard, H. F. (2001) A novel chromatin protein, distantly related to histone H2A, is largely excluded from the inactive X chromosome. *J. Cell Biol.* **152,** 375–384
11. Chadwick, B. P., and Willard, H. F. (2001) Histone H2A variants and the inactive X chromosome: identification of a second macroH2A variant. *Hum. Mol. Genet.* **10,** 1101–1113
12. Pehrson, J. R., and Fried, V. A. (1992) MacroH2A, a core histone containing a large nonhistone region. *Science* **257,** 1398–1400
13. Gautier, T., Abbott, D. W., Molla, A., Verdel, A., Ausio, J., and Dimitrov, S. (2004) Histone variant H2ABbd confers lower stability to the nucleosome. *EMBO Rep.* **5,** 715–720
14. Bao, Y., Konesky, K., Park, Y.-J., Rosu, S., Dyer, P. N., Rangasamy, D., Tremethick, D. J., Laybourn, P. J., and Luger, K. (2004) Nucleosomes containing the histone variant H2A.Bbd organize only 118 base pairs of DNA. *EMBO J.* **23,** 3314–3324
15. Doyen, C. M., Montel, F., Gautier, T., Menoni, H., Claudet, C., Delacour-Larose, M., Angelov, D., Hamiche, A., Bednar, J., Faiver-Moskalenko, C., Bouvet, P., and Dimitrov, S. (2006) Dissection of the unusual structural and functional properties of the variant H2A.Bbd nucleosome. *EMBO J.* **25,** 4234–4244
16. Okuwaki, M., Kato, K., Shimahara, H., Tate, S. I., and Nagata, K. (2005) Assembly and disassembly of nucleosome core particles containing histone variants by human nucleosome assembly protein I. *Mol. Cell. Biol.* **25,** 10639–10651
17. Malik, H. S., and Henikoff, S. (2003) Phylogenomics of the nucleosome. *Nat. Struct. Biol.* **10,** 882–891
18. Hall, T. A. (1999) BioEdit: a user-friendly biological sequence alignment editor and analysis program for Windows 95/98/NT. *Nucl. Acids Symp. Ser.* **41,** 95–98
19. Kumar, S., Tamura, K., and Nei, M. (2004) MEGA3: Integrated software for molecular evolutionary genetics analysis and sequence alignment. *Brief. Bioinform.* **5,** 150–163
20. Perez-Bercoff, A., Koch, J., and Burglin, T. R. (2006) LogoBar: bar graph visualization of protein logos with gaps. *Bioinformatics* **22,** 112–114
21. Nei, M., and Kumar, S. (2000) *Molecular Evolution and Phylogenetics,* Oxford University Press, New York
22. Zhang, J., Rosenberg, H. F., and Nei, M. (1998) Positive Darwinian selection after gene duplication in primate ribonuclease genes. *Proc. Natl. Acad. Sci. U. S. A.* **95,** 3708–3713
23. Saitou, N., and Nei, M. (1987) The neighbor-joining method: a new method for reconstructing phylogenetic trees. *Mol. Biol. Evol.* **4,** 406–425
24. Rzhetsky, A., and Nei, M. (1992) A simple method for estimating and testing minimum-evolution trees. *Mol. Biol. Evol.* **9,** 945–967
25. Felsestein, J. (1985) Confidence limits on phylogenies: an approach using the bootstrap. *Evolution Int. J. Org. Evolution* **39,** 783–791
26. Sitnikova, T. (1996) Bootstrap method of interior-branch test for phylogenetic trees. *Mol. Biol. Evol.* **13,** 605–611
27. Sitnikova, T., Rzhetsky, A., and Nei, M. (1995) Interior-branch and bootstrap tests of phylogenetic trees. *Mol. Biol. Evol.* **12,** 319–333
28. Frehlick, L. J., Eirin-Lopez, J. M., Jeffery, E. D., Hunt, D. F., and Ausio, J. (2006) The characterization of amphibian nucleoplasmins yields new insight into their role in sperm chromatin remodeling. *BMC Genomics* **7,** 99 [Published online April 28, 2006. doi: 10.1186/1471-2164-7-99]
29. Ausió, J., Dong, F., and van Holde, K. E. (1989) Use of selectively trypsinized nucleosome core particles to analyze the role of the

histone "tails" in the stabilization of the nucleosome. *J. Molec. Biol.* **206,** 451–463

30. Wang, X., Moore, S. C., Laszckzak, M., and Ausió, J. (2000) Acetylation increases the alpha-helical content of the histone tails of the nucleosome. *J. Biol. Chem.* **275,** 35,013–35,020

31. Thatchell, K., and van Holde, K. E. (1979) Nucleosome reconstitution: effect of DNA length on nucleosome structure. *Biochemistry* **18,** 2871–2880

32. Ausió, J., and Moore, S. C. (1998) Reconstitution of chromatin complexes from high-performance liquid chromatography-purified histones. *Methods* **15,** 333–342

33. Saperas, N., Chiva, M., Casas, M. T., Campos, J. L., Eirin-Lopez, J. M., Frehlick, L. J., Prieto, C., Subirana, J. A., and Ausio, J. (2006) A unique vertebrate histone H1-related protamine-like protein results in an unusual sperm chromatin organization. *FEBS J.* **273,** 4548–4561

34. Laemmli, U. K. (1970) Cleavage of structural proteins during the assembly of the head of bacteriophage T4. *Nature* **227,** 680–685

35. Li, A., Maffey, A. H., Abbott, D. W., Conde e Silva, N., Prunell, A., Siino, J., Churikov, D., Zalensky, A. O., and Ausió, J. (2005) Characterization of nucleosomes consisting of the human testis/sperm-specific histone H2B variant (hTSH2B). *Biochemistry* **44,** 2529–2535

36. Yager, T. D., and van Holde, K. E. (1984) Dynamics and equilibria of nucleosomes at elevated ionic strength. *J. Biol. Chem.* **259,** 4212–4222

37. Arents, G., and Moudrianakis, E. N. (1995) The histone fold: a ubiquitous architectural motif utilized in DNA compaction and protein dimerization. *Proc. Natl. Acad. Sci. U. S. A.* **92,** 11170–11174

38. Luger, K., Mader, A. W., Richmond, R. K., Sargent, D. F., and Richmond, T. J. (1997) Crystal structure of the nucleosome core particle at 2.8 A resolution. *Nature* **389,** 251–260

39. Marino-Ramirez, L., Kann, M. G., Shoemaker, B. A., and Landsman, D. (2005) Histone structure and nucleosome stability. *Expert. Rev. Proteomics* **2,** 719–729

40. Li, A., Eirín-López, J. M., and Ausió, J. (2005) H2AX: tailoring histone H2A for chromatin-dependent genomic integrity. *Biochem. Cell Biol.* **83,** 505–515

41. Greaves, I. K., Rangasamy, D., Devoy, M., Marshall Graves, J. A., and Tremethick, D. J. (2006) The X and Y chromosomes assemble into H2A.Z-containing facultative heterochromatin following meiosis. *Mol. Cell. Biol.* **26,** 5394–5405

42. Ausió, J., and van Holde, K. E. (1986) Histone hyperacetylation: its effects on nucleosome conformation and stability. *Biochemistry.* **25,** 1421–1428

43. Perry, M., and Chalkley, R. (1982) Histone acetylation increases the solubility of chromatin and occurs sequentially over most of the chromatin. A novel model for the biological role of histone acetylation. *J. Biol. Chem.* **257,** 7336–7347

44. Isenberg, I. (1978) *Histones*, Vol. 4, Part A, Academic Press, New York

45. Lewis, J. D., Song, Y., de Jong, M., Bagha, S., and Ausió, J. (2003) A walk though vertebrate and invertebrate protamines. *Chromosoma* **111,** 473–482

46. Retief, J. D., and Dixon, G. H. (1993) Evolution of protamine P2 genes in primates. *Eur. J. Biochem.* **218,** 1095

47. Rooney, A. P., and Zhang, J. (1999) Rapid evolution of a primate sperm protein: relaxation of functional constraint or positive Darwinian selection? *Mol. Biol. Evol.* **16,** 706–710

48. Wyckoff, G. J., Wang, W., and Wu, C. I. (2000) Rapid evolution of male reproductive genes in the descent of man. *Nature* **403,** 304–309

49. Eirín-López, J. M., González-Tizón, A. M., Martínez, A., and Méndez, J. (2004) Birth-and-death evolution with strong purifying selection in the histone H1 multigene family and the origin of *orphon* H1 genes. *Mol. Biol. Evol.* **21,** 1992–2003

50. Levchenko, V., and Jackson, V. (2004) Histone release during transcription: NAP1 forms a complex with H2A and H2B and facilitates a topologically dependent release of H3 and H4 from the nucleosome. *Biochemistry* **43,** 2359–2352

51. Calestagne-Morelli, A., and Ausio, J. (2006) Long-range histone acetylation: biological significance, structural implications, and mechanisms. *Biochem. Cell Biol.* **84,** 518–527

52. Garcia-Ramirez, M., Rocchini, C., and Ausio, J. (1995) Modulation of chromatin folding by histone acetylation. *J. Biol. Chem.* **270,** 17923–17928

53. Norton, V. G., Imai, B. S., Yau, P., and Bradbury, E. M. (1989) Histone acetylation reduces nucleosome core particle linking number change. *Cell* **57,** 449–457

54. Clayton, A. L., Hazzalin, C. A., and Mahadevan, L. C. (2006) Enhanced histone acetylation and transcription: a dynamic perspective. *Mol. Cell* **23,** 289–296

55. Luger, K., and Richmond, T. J. (1998) DNA binding within the nucleosome core. *Curr. Opin. Struct. Biol.* **8,** 33–40

56. Dorigo, B., Schalch, T., Bystricky, K., and Richmond, T. J. (2003) Chromatin fiber folding: requirements for the histone H4 N-terminal tail. *J. Mol. Biol.* **327,** 85–96

57. Angelov, D., Verdel, A., An, W., Bondarenko, V., Hans, F., Doyen, C. M., Studitsky, V. M., Hamiche, A., Roeder, R. G., Bouvet, P., and Dimitrov, S. (2004) SWI/SNF remodeling and p300-dependent transcription of histone variant H2ABbd nucleosomal arrays. *EMBO J.* **23,** 3815–3824